TOXICOLOGICAL SCIENCES **51,** 126–134 (1999)

Application of Laser Scanning Confocal Microscopy in the Analysis of Particle-Induced Pulmonary Fibrosis

James M. Antonini,*[,1] Tina G. Charron,* Jenny R. Roberts,† Jean Lai,† Terri L. Blake,* and Rick A. Rogers†

**Health Effects Laboratory Division, National Institute for Occupational Safety and Health, Morgantown, West Virginia 26505; and †Physiology Program, Harvard School of Public Health, Boston, Massachusetts 02115*

Received December 15, 1998; accepted April 25, 1999

Laser scanning confocal microscopy (LSCM) allows us to simultaneously quantitate the degree of lung fibrosis and distinguish various pathological lesions of intact lung tissue. Lucifer Yellow has been shown an ideal fluorescent stain to examine the connective tissue matrix components of embedded lung tissue with LSCM. We evaluated the use of LSCM in quantitating lung fibrosis and compared this procedure with the more traditional method of assessing fibrosis by measuring hydroxyproline, a biochemical assay of collagen. CD/VAF rats were intratracheally dosed with silica (highly fibrogenic), Fe_2O_3 (non-fibrogenic), and saline (vehicle control) at a high dose of 10-mg/100 g body weight. At 60 days post-instillation, the left lung was dissolved in 6 M HCl and assayed for hydroxyproline. Silica induced increases of 58% and 94% in hydroxyproline content over the Fe_2O_3 and control groups, respectively. The right lung lobes were fixed, sectioned into blocks, dehydrated, stained with Lucifer Yellow (0.1 mg/ml), and embedded in Spurr plastic. Using LSCM and ImageSpace software, the tissue areas of ten random scans from ten blocks of tissue for each of the three groups were measured, and three-dimensional reconstructions of random areas of lung were generated. The silica group showed increases of 57% and 60% in the lung areas stained by Lucifer Yellow over the Fe_2O_3 and control groups, respectively. Regression analysis of hydroxyproline vs. lung tissue area demonstrated a significant positive correlation ($p < 0.05$) with a correlation coefficient of 0.91. Histological analysis of right lung tissue revealed a marked degree of granulomatous interstitial pneumonitis for the silica group, which was absent in the Fe_2O_3 and control groups. No significant differences ($p < 0.05$) in hydroxyproline content and measured tissue area were observed between the Fe_2O_3 and control groups. LSCM, and its associated advanced image analysis and three-dimensional capabilities, is an alternative method to both quickly quantitate and examine fibrotic lung disease without physical disruption of the tissue specimen.

Key Words: **confocal microscopy; lung fibrosis; silica; Lucifer Yellow; hydroxyproline.**

Many toxic agents damage the delicate structure of the lungs and produce an increase in connective tissue, causing pulmonary fibrosis (Witschi *et al.*, 1985). These fibrotic lesions are characterized by an abnormal accumulation of collagen. The most common way to quantitate pulmonary fibrosis is to estimate lung collagen content by hydrolysis of the entire lung or a single lobe in a strong acid. Hydroxyproline, an amino acid found exclusively in collagen, is subsequently measured by conventional colorimetric methods (Haschek and Witschi, 1979; Witschi *et al.*, 1985). This procedure is somewhat tedious, takes several days to complete, and does not alone distinguish areas of fibrotic lesions. Histology is also needed to provide additional important information. With laser scanning confocal microscopy (LSCM), we have developed a procedure that allows both qualitative and quantitative assessment of pulmonary fibrosis without physical disruption of the lung tissue sample.

LSCM offers many advantages over conventional microscopic techniques (Wright *et al.*, 1993). The shallow depth of field of confocal microscopes allows information to be collected from a well-defined optical section, rather than from most of the specimen, as in the conventional light microscope. Consequently, out-of-focus light is virtually eliminated, resulting in an increase in contrast, clarity, and detection sensitivity (Inoue, 1989; Shotten, 1989). The confocal microscope optically sections specimens so that physical sectioning artifacts observed with conventional light and electron microscopy are eliminated. Stacks of optical sections taken at successive focal planes can be reconstructed to produce a three-dimensional view of the specimen (Wilson, 1989). The basic image analysis and display systems integrated with the commercially available LSCMs provide ease of operation, rapid image formation, and digital image collection for morphometric analysis (Pawley, 1989; Shotten, 1989; Smith *et al.*, 1991).

For this investigation, we evaluated the use of LSCM in quantitating particle-induced lung fibrosis and compared this procedure with the more traditional methods of assessing fibrosis by weighing recovered lungs and measuring hydroxyproline. CD/VAF rats were intratracheally dosed with a highly fibrogenic dust, crystalline silica, and a relatively inert, non-fibrogenic dust, Fe_2O_3, at a high particle dose of 10 mg/

[1] To whom correspondence should be addressed at Health Effects Laboratory Division, National Institute for Occupational Safety and Health, 1095 Willowdale Road (M/S 2015), Morgantown, WV 26505. Fax: (304) 285-5938. E-mail: jga6@cdc.gov.

100 g body weight. The lungs were examined for fibrosis 60 days later. It has been well documented that inhalation of crystalline silica results in inflammation, damage to the respiratory epithelium and interstitial matrix, and fibrosis (Bowden, 1987; Lapp and Castranova, 1993). The examination of lungs from workers and experimental animals after exposure to Fe_2O_3 have demonstrated minimal lung damage, a lack of complicated pulmonary lesions, and no progressive massive fibrosis (Antonini *et al*., 1996; Beck *et al*., 1982; Sferlazza and Beckett, 1991). To image exposed lungs with LSCM, the lungs were fixed, sectioned into blocks, dehydrated, stained with a fluorescent dye (Lucifer Yellow), and embedded in Spurr plastic. We have shown previously that Lucifer Yellow is an ideal fluorescent stain that is resistant to photo-bleaching, for examining the connective tissue of embedded lungs with LSCM (Antonini *et al*., 1996; Oldmixon *et al*., 1994; Oldmixon and Carlsson, 1993; Rogers *et al*., 1992). Lucifer Yellow-stained lung parenchyma was randomly scanned using LSCM, and the area of the connective tissue matrix within the alveolar walls stained by Lucifer Yellow was measured.

MATERIALS AND METHODS

Materials. Crystalline Min-U-Sil silica (U.S. Silica Corp., Berkeley Springs, WV) was 99.5% alpha quartz as determined by X-ray diffractrometry with a count mean diameter of 3.5 μm. Before use, the silica was boiled in 1.0 M HCl for 60 min to remove any surface contaminants, then washed, dried, and sterilized. Fe_2O_3 particles (gamma-Fe_2O_3) were produced by the combustion of iron pentacarbonyl [$Fe(CO)_5$] vapors as described by Valberg and Brain (1979). The resulting iron oxide particle agglomerates had a count mean diameter of 0.87 μm. Lucifer Yellow-CH was obtained from Molecular Probes (Eugene, OR). Unless otherwise specified, other reagents were obtained from Sigma Chemical Company (St. Louis, MO).

Animals. Male CD/VAF rats weighing 200–250 g were used for all experiments (Charles River Laboratories, Wilmington, MA). They were given a conventional laboratory diet and tap water *ad libitum* and were housed in a clean air, viral- and antigen-free room with restricted access.

Intratracheal Instillation. Rats (n = 3–4/treatment group) were intratracheally instilled with 10 mg of silica (fibrogenic particle) and Fe_2O_3 (non-fibrogenic particle) suspended in 150 μl of 0.9% sterile saline/100 g body weight. In a previous study, we have shown that silica induces pulmonary fibrosis at this dose (Blake *et al*., 1996). Animals in the vehicle control group were intratracheally dosed with 150 μl of 0.9% sterile saline/100 g body weight.

Before the intratracheal instillation procedure, the rats were lightly anesthetized by an intraperitoneal injection of 0.6 ml of 1% sodium methohexital (Brevital, Eli Lilly Co., Indianapolis, IN). The instillations were performed according to a method reported by Brain *et al*. (1976). Before instillation, the particle samples were sonicated for 1 min.

Assessment of Fibrosis

At 60 days post-instillation, animals were given an overdose of sodium pentobarbital and exsanguinated by severing the abdominal aorta. After the trachea was cannulated and removed along with lungs, the left lung was ligated, removed, weighed, and frozen immediately at –70°C for later determination of hydroxyproline, a biochemical index of fibrosis. The right lung lobes were preserved with 2.5% glutaraldehyde by airway gravity fixation at a pressure of 30-cm water. We felt this to be the best method to ensure maximal lung inflation and eliminate any potential variability in inflation from animal to animal. Gil *et al*. (1979) has demonstrated that inflating the lungs with saline at >10-cm water pressure, a total lung capacity of over 90% was reached. The trachea was ligated so the cannula could be cut away, and the lung samples were stored in the glutaraldehyde until processed for histopatholgy.

Hydroxyproline. Lung hydroxyproline was measured as an index of pulmonary fibrosis. Frozen left lung samples were thawed and minced, then processed and analyzed according to the method of Witschi *et al*. (1985). Briefly, chopped lung samples were hydrolyzed in 6 M HCl for 72 h, then neutralized with NaOH. Aliquots of the hydrosylate were diluted in borate-alanine buffer and oxidized with chloramine T. The reaction was stopped with sodium thiosulfate, toluene was added, and the samples were boiled. After centrifugation, an aliquot of the organic phase was added to Ehrlich's reagent. Absorbance was read at 560 nm on a Gilford Spectrophotometer. Micrograms of hydroxyproline per left lung were calculated from a standard curve.

Microscopy. Histopathological evaluation was accomplished by sectioning fixed right lung lobes which had been dehydrated and embedded in paraffin, and then stained with hematoxylin and eosin. Remaining fixed right lung tissue was cut into blocks (~10 mm), dehydrated in a graded series of ethanol washes, fluorescently labeled with a 0.1 mg/ml concentration of Lucifer Yellow-CH, incubated for 24 hr, and then embedded in Spurr's epoxy for analysis by confocal microscopy (Rogers *et al*., 1992).

Confocal microscopy. Images were recorded using a Sarastro 2000 (Molecular Dynamics, Inc., Sunnyvale, CA) laser scanning confocal microscope (Optiphot-2, Nikon, Inc., Melville, PA) fitted with an argon-ion laser. Emission spectra >510 nm were diverted to a separate photodetector and used to image lung tissue and cells. Reflected light <510 nm was simultaneously passed to a separate optical path and provided images of instilled particles. Images of lung tissue and mineral particles were combined to reveal the position of particles among lung structures. A $\frac{1}{4}$ wavelength polarizing filter was placed in the optical path to maximize the reflected light signal from the mineral particles.

Using a 40× objective, we randomly scanned 10 sections of lung parenchyma, excluding large airways, from each of 10 blocks of tissue for each animal from the 3 groups. An image field 512 μm × 512 μm (2.62 × 10^5 μm^2) was defined over a region of parenchyma entirely filling the field. With the ImageSpace software (Molecular Dynamics, Inc., Sunnyvale, CA), we determined the threshold pixel-intensity levels that defined Lucifer Yellow-positive and Lucifer Yellow-negative sites, and thus identified the presumed connective tissue matrix components. To set the threshold, we interactively probed the images using a sliding gradient color map to effectively determine the intensity ranges of specific structures: 0–12 pixel intensity units for air space, 13–37 pixel intensity units for air space cells and debris, and >38 pixel intensity units for connective tissue matrix components. Fluorescent signals below a pixel intensity value of 38 were thresholded out, which eliminated the measurement of nearly all the cells and debris within the air spaces. If inflammatory cells were present within the air spaces after the threshold was established, a masking tool associated with the software was used to eliminate the cells from the area measurements. All random scans of the lung tissue, for each treatment group, were recorded ~3–5 μm from the top of the tissue block at the same photo multiplier tube (PMT) setting of 450, pinhole aperture setting of 50 μm, and at the same laser voltage setting of 20 mW. This analysis resulted in a data set expressed as connective tissue (Lucifer Yellow-positive) area in μm^2 per image field. Randomly selected airways from embedded tissue of the different treatment groups were later scanned, and 3-dimensional projections were generated from serial optical sections of lung tissue. Three-dimensional reconstruction was generated using Voxel View Ultra software (Vital Images, Inc., Fairfield, IA).

Statistical Analysis. Results are expressed as means ± standard error of measurement (SE). Statistical analyses were carried out with the Statview statistical program (Abacus Concepts, Inc., Berkeley, CA). For all parameters, an analysis of variance (ANOVA) was performed. If a significant interaction was present, the significance between each of the individual groups was analyzed using the Fischer's Least Significance Difference post-hoc test. Regression analysis of hydroxyproline from biochemical measurements vs.

TABLE 1
Total Body and Left Lung Weights

Treatment groups	Total body weight (g)	Left lung weight (g)	Left lung/total body weight
Saline	540.2 ± 24.8	0.693 ± 0.08	1.29×10^{-3}
Fe_2O_3	476.8 ± 2.92	0.633 ± 0.03	1.33×10^{-3}
Silica	498.0 ± 11.9	1.53 ± 0.09*	3.09×10^{-3}*

Note. Body weight values are means ± SE.
*Significantly greater than other groups, $p < 0.05$.

lung area stained by Lucifer Yellow from LSCM analysis was performed to determine if a positive correlation existed between the two parameters. For all analyses, the criterion of significance was $p < 0.05$.

RESULTS

As a gross measure of lung damage, the left lung weights and the ratio of left lung weight to body weight were determined for each group (Table 1). The intratracheal instillation of silica induced significant increases greater than 2-fold in both left lung weight and the ratio of left lung weight to body weight when compared to the Fe_2O_3 and saline groups. Silica caused increases of 58% and 94% in hydroxyproline content, a biochemical measure of fibrosis, over the Fe_2O_3 and saline groups, respectively (Fig. 1).

Histopathological evaluation further confirmed the fibrotic response associated with the intratracheal instillation of silica (Fig. 2). Lung changes after exposure to saline and Fe_2O_3 group were minimal (Figs. 2A and 2B). Localized areas of Fe_2O_3 particle-containing macrophages were observed in the terminal bronchioles and alveolar ducts (Fig. 2B, arrows). The response to silica was characterized by marked granulomatous interstitial pneumonitis and alveolar histioctyosis (Figs. 2C and 2D).

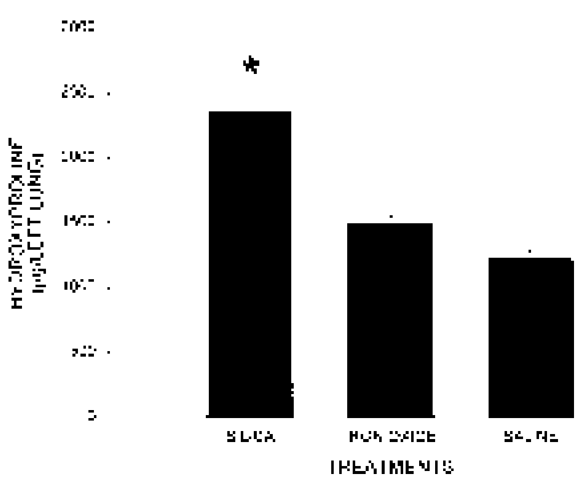

FIG. 1. Hydroxyproline content of left lung 60 days post-instillation of silica, Fe_2O_3, and saline (vehicle control). The animals received a single particle dose of 10 mg/100 g body wt. Values are means ± SE. Mean value of the silica group was significantly greater than the values of the other groups, *$p < 0.05$.

Lung tissue *en bloc* stained with Lucifer Yellow was examined to determine whether this fluorochrome was appropriate for use in this study (Fig. 3). Lung parenchyma of a saline control rat was easily imaged after Lucifer Yellow treatment (Fig. 3A). A high intratracheal dose of silica (10 mg/100 g body weight) caused a massive influx of inflammatory cells, cellular debris, and extracellular phospholipid into the alveolar spaces, all of which were fluorescently labeled by Lucifer Yellow (Fig. 3B). However, Lucifer Yellow produced differential fluorescent staining of connective tissue and pulmonary cells and debris. Connective tissue elements in alveolar walls (Fig. 3C, arrows) were clearly visible, having a higher fluorescent intensity than the lung macrophages in the alveolar spaces. Using the reflected light capabilities of LSCM, instilled particles could also be observed among lung structures (Fig. 4). Numerous accumulations of Fe_2O_3 particles were easily imaged in lung tissue 60 days post-instillation. The majority of Fe_2O_3 particles present in the lungs were found within lung macrophages (Figs. 4A and 4B, arrows).

For quantitation of the fibrotic response, lung tissue from the 3 different treatment groups were randomly scanned at exactly the same PMT, pinhole aperture, and laser voltage settings. The number of pixels within the image area that demonstrated brightness intensity above a defined threshold were considered positive for Lucifer-Yellow staining. They were summed to calculate the total connective tissue area in μm^2 per image area, using an ImageSpace software package associated with the LSCM. In Figure 5, we show representative confocal micrographs of lung parenchyma from the 3 different treatment groups. Background areas are displayed in purple (air spaces), low intensity sites (tissue autofluorescence) appear blue, and increasingly high intensity areas are displayed as green, yellow, red, or white with a pixel intensity scale of 0–255. Lungs appear normal for both the saline control and iron oxide groups, demonstrating a few bright lines of connective tissue in alveolar septae (Figs. 5A and 5B). Lung sections from silica-exposed rats revealed diffuse thickening of the alveolar walls with the extensive bright regions of fluorescence (Fig. 5C). Silica caused significant increases of 57% and 60% in lung tissue area

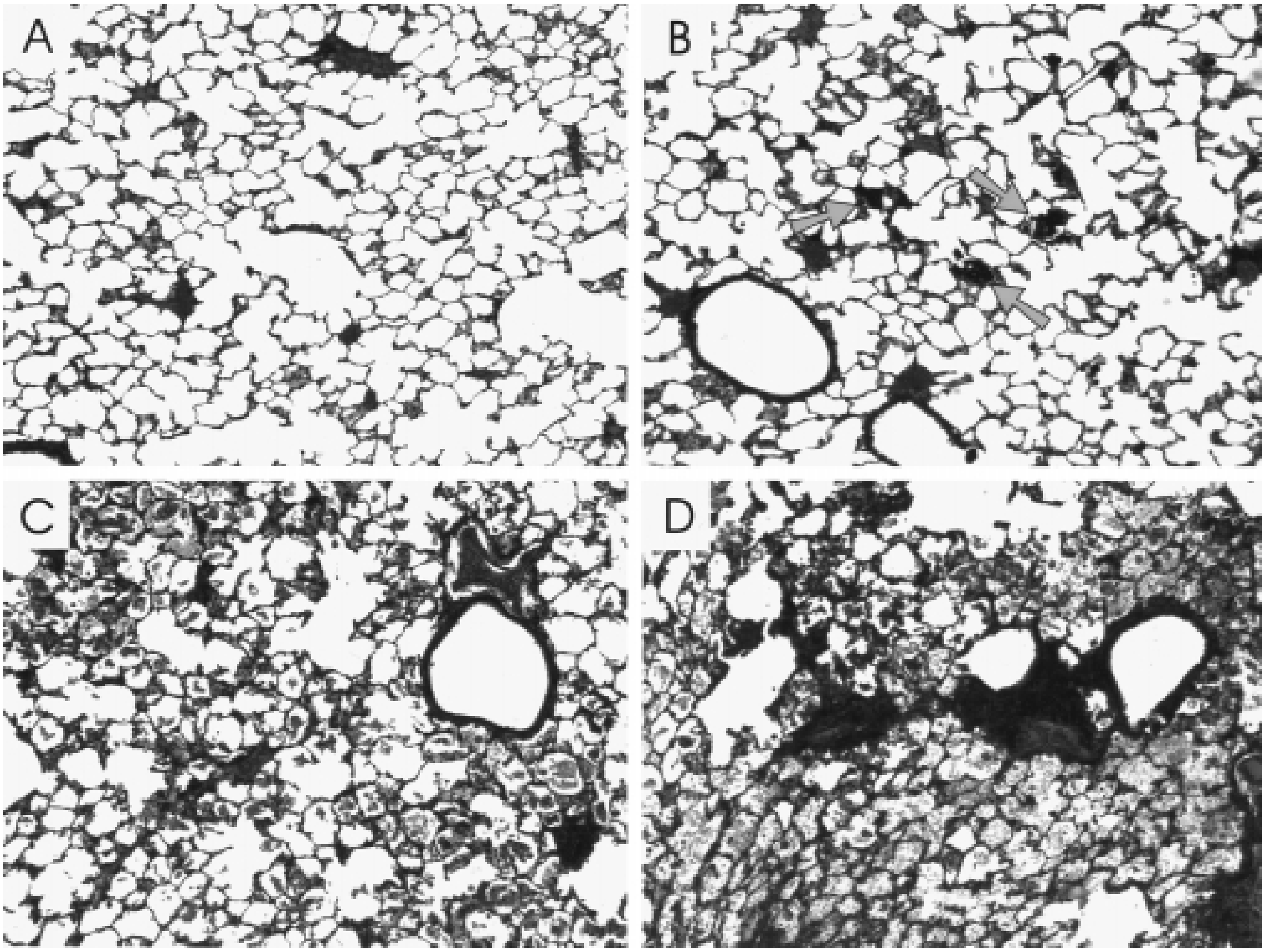

FIG. 2. Light micrograph of hematoxylin- and eosin-stained right lung 60 days post-instillation of (A) saline, (B) Fe_2O_3, and (C, D) silica. The animals received a single particle dose of 10 mg/100 g body wt. Saline was used as vehicle control. Fe_2O_3 particles were observed in lung macrophages (B: arrows).

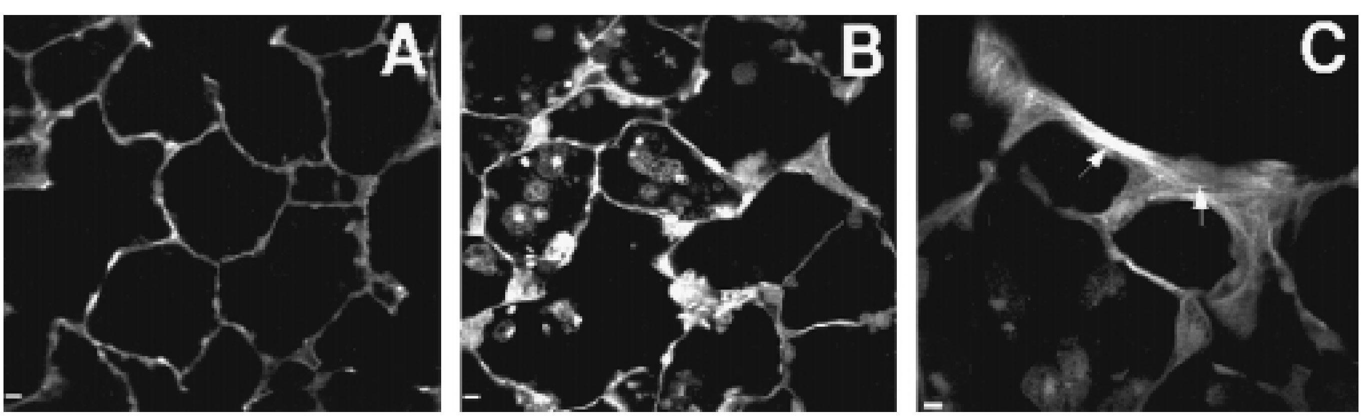

FIG. 3. Confocal micrograph of Lucifer Yellow-stained right lung tissue 60 days post-instillation of (A) saline and (B, C) silica. The animals received a single particle dose of 10 mg/100 g body wt. Saline was used as vehicle control. Collagen fibers in alveolar walls are easily observed (C: arrows). Bar is 10 μm in A and B and 5 μm in C.

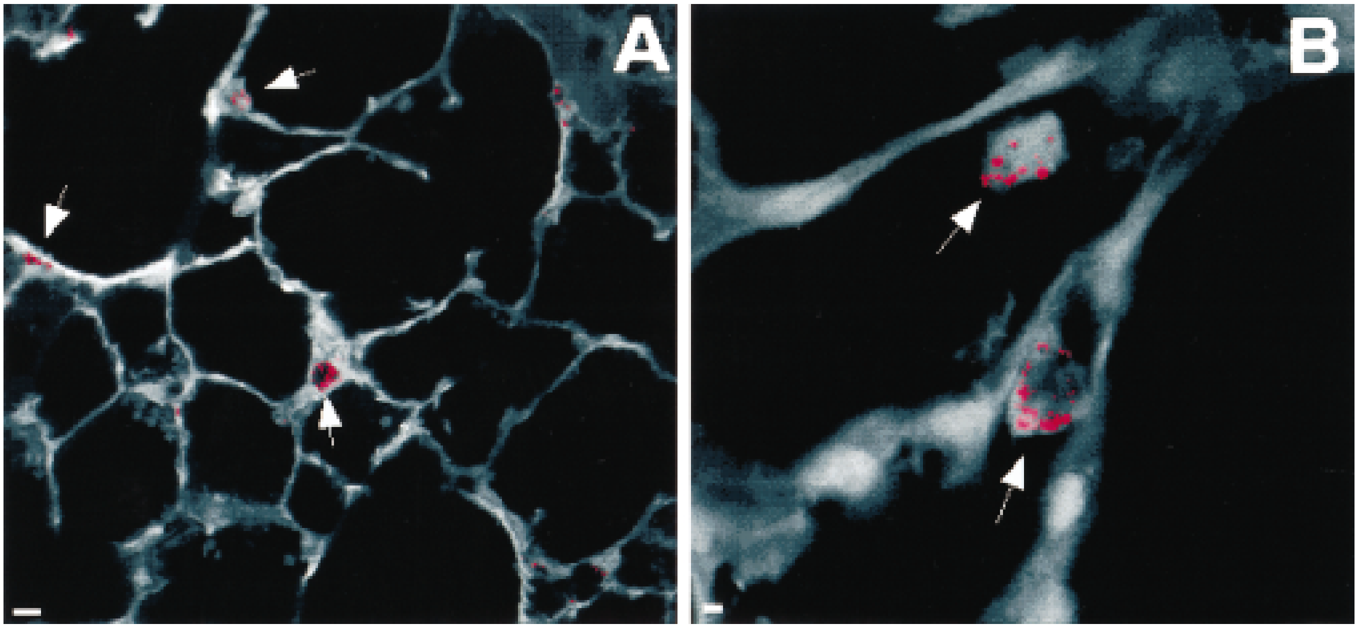

FIG. 4. Confocal micrograph of Lucifer Yellow-stained right lung tissue 60 days post-instillation of Fe_2O_3. The animals received a single particle dose of 10 mg/100 g body wt. Fe_2O_3 particles (red) are observed within lung macrophages (A,B: arrows) Bar is 10 μm in A and 2 μm in B.

stained by Lucifer Yellow when measured by LSCM analysis, as compared to the Fe_2O_3 and control groups, respectively (Fig. 6). Regression analysis of hydroxyproline from biochemical measurements vs. lung tissue area from LSCM analysis demonstrated a significantly positive correlation ($p < 0.05$) with a correlation coefficient of 0.91 (Fig.7).

Since there is no physical disruption of the lung tissue with LSCM, different areas of tissue within the same lobe of lung can both be examined histologically and quantified. Two areas of lung parenchyma from the same lung lobe from a rat exposed to silica were compared (Fig. 8). In Figure 8A, a silicotic nodule in the granulomatous phase was observed. The lesion is composed predominately of histiocytic cells and collagen fibers. The lung area section that is stained by Lucifer Yellow for this imaged region was $4.92 \times 10^4\ \mu m^2$. In Figure 8B, an area of less damage is shown. An infiltration of inflammatory cells and cellular debris is seen in the alveolar spaces. While alveolar thickening is observed, the lung area section

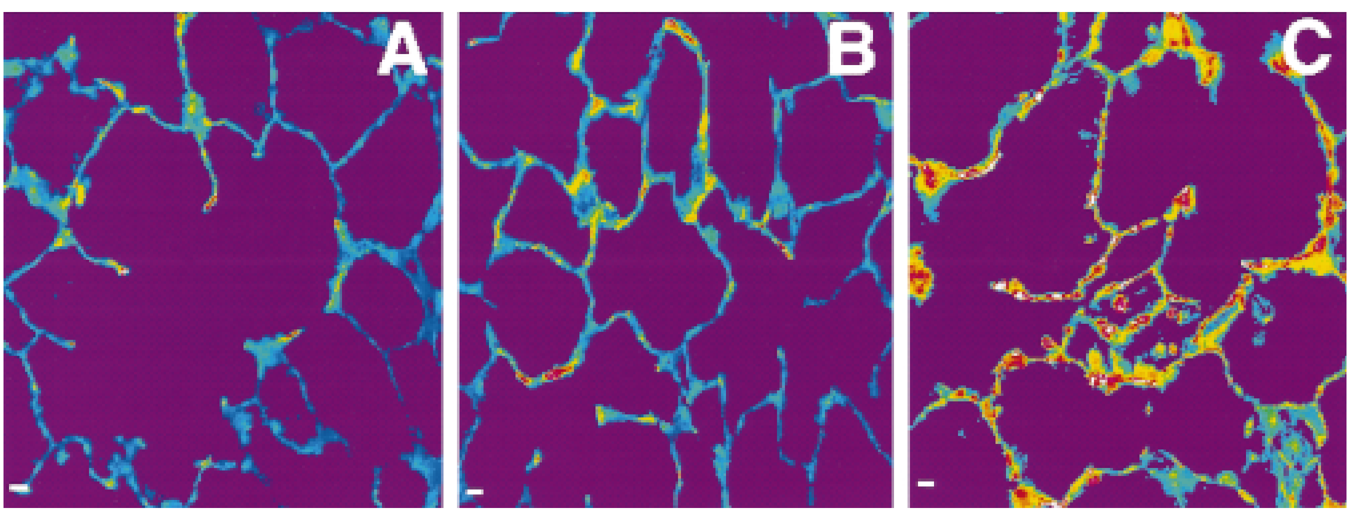

FIG. 5. Confocal micrograph of Lucifer Yellow-stained right lung tissue 60 days post-instillation of (A) saline, (B) Fe_2O_3, and (C) silica. The animals received a single particle dose of 10-mg/100 g body wt. Saline was used as vehicle control. The pixel intensity was divided into scaled cohorts, and each cohort was assigned a color. Background areas are displayed in purple, low intensity sites appear blue, and increasingly high intensity areas are displayed as green, yellow, red, or white. Bar is 10 μm.

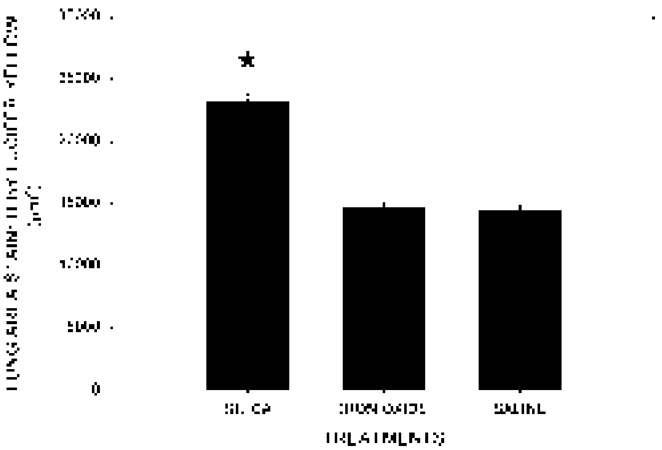

FIG. 6. Measured tissue area of random LSCM scans of Lucifer Yellow-stained right lung tissue 60 days post-instillation of silica, Fe_2O_3, and saline (vehicle control). The animals received a single particle dose of 10 mg/100 g body wt. Values are means ± SE. Mean value of the silica group was significantly greater than the values of the other groups, *$p < 0.05$.

stained by Lucifer Yellow was only 2.35×10^4 μm^2, which is more than 2 times less than that seen in Figure 8A.

Three-dimensional projection series of airways and parenchyma from Lucifer Yellow-stained rat lung could be rendered *en bloc* (Fig. 9). Three-dimensional images of lung tissue 67.5 μm (Fig. 9A) and 112.5 μm (Fig. 9B) thick were rendered. A definitive thickening of the alveolar septa (Figs. 9A and 9B, arrows) and the massive accumulation of inflammatory cells, cellular debris, and extracellular phospholipid in the alveolus (Figs. 9A and 9B) of the silica-treated rats were easily observed as compared to the saline group.

DISCUSSION

We have introduced the use of LSCM to assess particle-induced pulmonary fibrosis. LSCM optics remove flare emitted in the plane of focus and reject out-of-focus light from underlying and overlying structures of a sample (Wright *et al.*, 1993). Only the point of focus is recorded. Rejection of out-of-focus light allows optical sectioning of the sample without physical disruption of the specimen, permitting large areas of lung to be studied without sacrificing resolution. Using basic image analysis and morphometric procedures, LSCM is, therefore, a potentially powerful tool for quantitative studies.

The most commonly used method to quantitate fibrotic lesions in the lung is to estimate collagen content by measuring hydroxyproline. This biochemical procedure is time consuming, labor intensive, and requires entire lungs for accurate analysis. It is most appropriate to express lung hydroxyproline on a per lung basis, e.g., as total mass, rather than on a per wet or dry weight basis, e.g., as concentrations (Witschi *et al.* 1985). Using an animal model of pulmonary fibrosis, Haschek *et al.* (1982) calculated hydroxyproline mass and found that fibrotic lungs, over a one-year period, consistently had significantly higher amounts of total hydroxyproline than lungs of appropriate controls. However, when collagen from the same animals was calculated as hydroxyproline concentrations, initially there was a decrease of hydroxyproline compared to controls. At later time points, the differences between treated and control animals were not significant. Lung weight usually increases with inflammation, edema, and fibrosis. Thus, expression of lung hydroxyproline per weight may underestimate the degree of collagen accumulation that has occurred. Unfortunately, it is not always possible to calculate hydroxyproline per total lung, especially if human lung biopsy samples are to be assessed. Additional methods to quantify pulmonary fibrosis are thus needed.

For the accurate measurement of hydroxyproline, entire lungs or single lung lobes need to be digested. The ability to identify pulmonary lesions and determine their location in the lungs is then lost. The nature and localization of certain lesions may be important in assessing the development, progression, and result of fibrosis. In a study by Hakkinen *et al.* (1983), rats were administered either oleic acid or a combination of bleomycin and 80% oxygen. Both treatments induced fibrosis at 3 weeks, as determined by hydroxyproline measurement. However, the histopathological lesions were different. Intravenous injection of oleic acid resulted in focal areas of total destruction of pulmonary parenchyma, which healed by fibrosis of the infarcted region with the remaining lung being normal. Treatment with bleomycin and hyperoxia resulted in an increase in interstitial inflammatory cells and collagen with diffuse involvement of the alveolar walls, while maintaining architec-

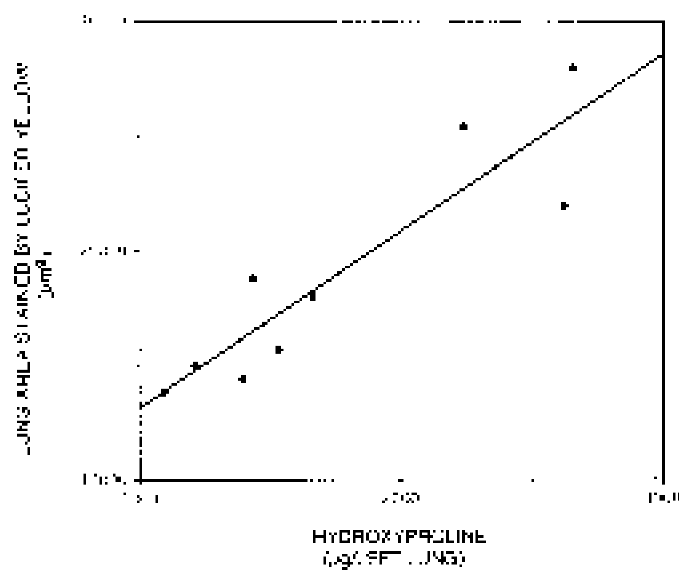

FIG. 7. Regression analysis of hydroxyproline from biochemical measurements vs. lung area stained by Lucifer Yellow from LSCM analysis. The line represents the linear regression line of best fit for all data points. A significant positive correlation ($p < 0.05$) between the two parameters was observed with a correlation coefficient of 0.91.

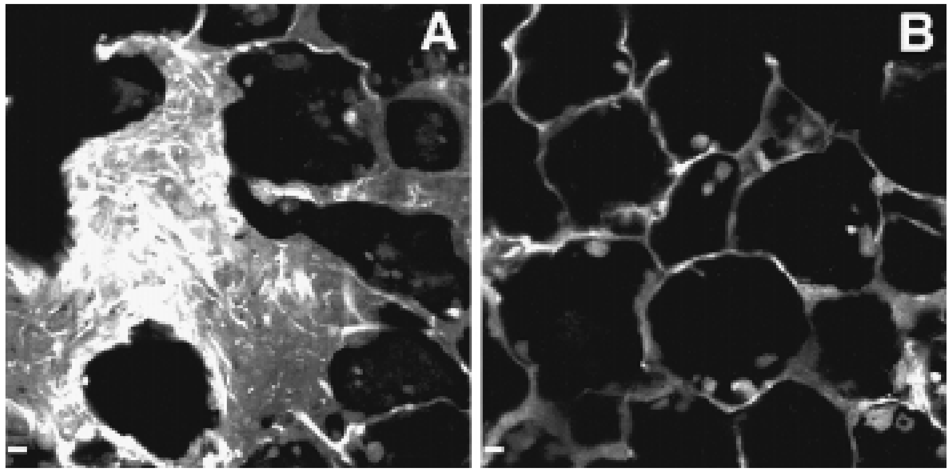

FIG. 8. Confocal micrograph of Lucifer Yellow-stained right lung tissue 60 days post- instillation of silica (A and B). The animals received a single particle dose of 10 mg/100 g body wt. Bar is 10 μm.

tural integrity. It was then concluded that the two treatments and the resulting lesions would have different effects on pulmonary gas exchange.

In another study, Haschek *et al*. (1982) showed that intraperitoneal injections of either butylated hydroxytoluene (BHT) or cyclophosphamide both decreased lung compliance and increased total lung hydroxyproline that persisted for one year, as compared to controls. However, the pulmonary lesions were quite different. Early after treatment with BHT, there was a diffuse interstitial pneumonitis with collagen deposition in the thickened alveolar septa. After one year, the BHT-induced pneumonitis disappeared and the lungs looked normal, although biochemical measurements showed those increased quantities of collagen persisted in the treated lungs. On the other hand, cyclophosphamide induced a multifocal alveolar accumulation of macrophages, which was present at 3 weeks post-treatment. These lesions had increased in number and size one year after treatment. A procedure then is needed which allows both qualitative and quantitative assessment of pulmonary fibrosis without physical disruption of the lung tissue sample.

In this current investigation, rats were intratracheally instilled with a high dose (10 mg/100 g body weight) of either silica (fibrogenic, highly inflammatory) or Fe_2O_3 (non-fibro-

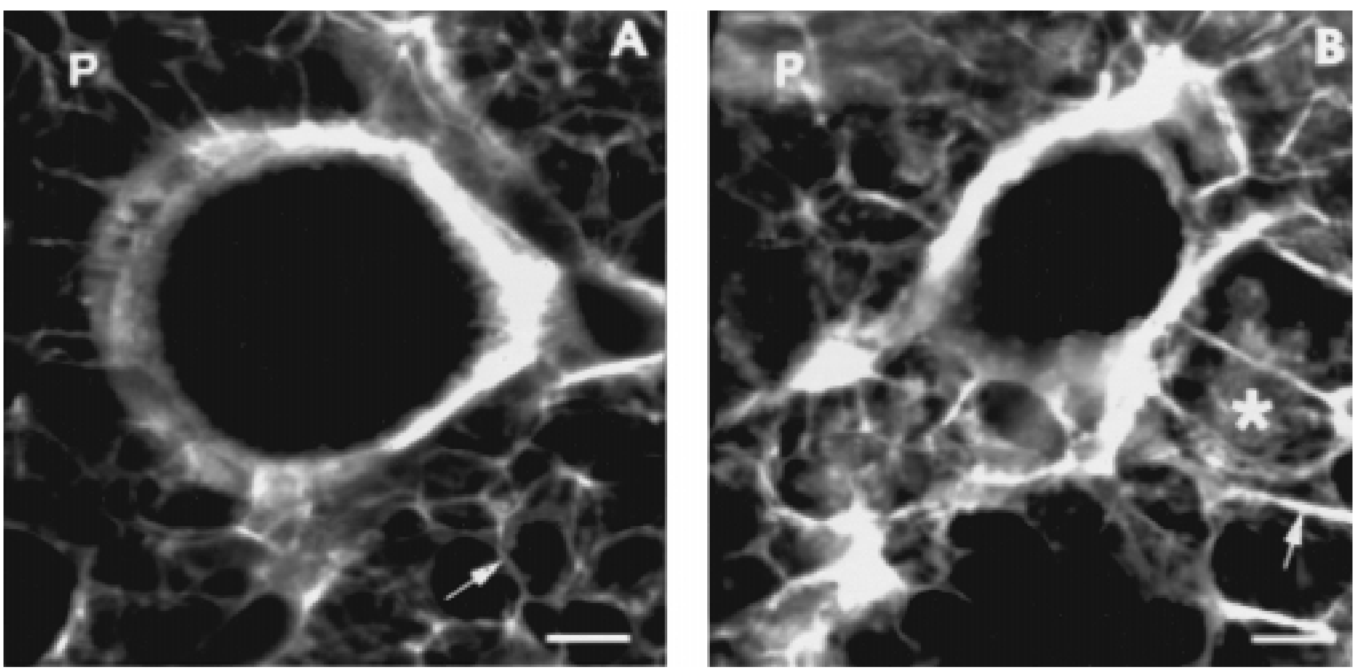

FIG. 9. Three-dimensional projection series of an airway from right lung tissue 60 days post-instillation of (A) saline and (B) silica. The animals received a single particle dose of 10 mg/100 g body wt. Images were rendered from 150 serial sections which were 0.45 μm thick (67.5 μm) and 173 serial sections which were 0.65 μm thick (112.5 μm). P is parenchyma; * is inflammatory cells and debris in alveolus; arrow points to alveolar septum; and Bar is 50 μm.

genic) particles. Lungs were removed and imaged after labeling with the fluorochrome, Lucifer Yellow. Large areas of exposed lung tissue *en bloc* were randomly scanned using LSCM. Fibrosis was quantified by measuring the tissue area from images of randomly scanned, fluorescently-labeled lungs generated for each treatment group. Lucifer Yellow has been used in a previous study to visualize large volumes of lung tissue using LSCM (Oldmixon and Carlsson, 1993). Rogers *et al*. (1992) have demonstrated that elastin, collagen, and other cellular components of lungs treated with Lucifer Yellow were easily distinguished, measured, and reconstructed three-dimensionally. Connective tissue components were easily identified in alveolar walls of lungs from each of the treatment groups used in this study. Threshold pixel-intensity levels were established and identified for the connective tissue matrix components. Connective tissue area stained by Lucifer Yellow was then determined while the extracellular phospholipid, inflammatory cells, and cellular debris present in the air spaces were excluded from measurement.

The instillation of silica caused increases of 57 and 60% in measured lung area stained by Lucifer Yellow compared to the Fe_2O_3 and control groups, respectively. These increases were comparable to what was observed in the measurement of hydroxyproline. Silica caused increases of 58 and 94% in hydroxyproline content over the Fe_2O_3 and saline groups, respectively. Regression analysis of hydroxyproline vs. lung area stained by Lucifer Yellow demonstrated a significant positive correlation with a correlation coefficient of 0.91. The increases in both Lucifer Yellow-stained lung tissue area and hydroxyproline seen for silica were indicative of a fibrotic response and statistically significant when compared to the Fe_2O_3 and saline groups. No significant differences were observed between the Fe_2O_3 and saline groups for either lung tissue area or hydroxyproline content.

It is important to emphasize that Lucifer Yellow is not specific for collagen but specific for the lung connective tissue matrix components. We can conclude from this study that measuring the area of tissue stained by Lucifer Yellow is another method for quantifying pulmonary fibrosis. Our results correlate well with the standard method to quantify fibrosis by measuring hydroxyproline. In a similar study, Malkusch *et al*. (1995) used the fluorochrome Sirius red to quantify lung collagen and measure the percent of tissue occupied by Sirius red staining in their determination of fibrosis. They also showed corresponding results in comparing lung tissue measurements using both colorimetric and morphometric determinations. Our study differed from the Malkusch study in that we used a different fluorescent probe and utilized LSCM, while they used conventional light microscopy.

Also of importance for the measurement of hydroxyproline, the entire left lung was digested and the airways, parenchyma, and pleura were sampled in our study. In the confocal microscopy studies, only the parenchyma and pleura were randomly sampled. We specifically excluded large airways because the particles were delivered to the deep areas of the lungs by intratracheal instillation. Fibrotic lesions that appear after silica exposure occur at the site of deposition. Thus, we felt we would see little change in connective tissue of the large airways at the subchronic time point of 60 days using this route of particle administration in this study. Malkusch *et al*. (1995) found little change by morphometric measurements in % collagen when entire lungs were sampled between groups which showed fibrotic lesions and those that did not. When the bronchial regions were excluded, they observed a significant increase in collagen content in the lung samples with fibrotic lesions. They then concluded that the increase in collagen content was restricted exclusively to the alveolar regions of the lungs.

In addition to quantifying the fibrotic response within a specific tissue sample, we were able to histologically assess the type of damage associated with the different particle treatment, within the same tissue specimen, due to the optical sectioning capability of LSCM. Since the tissue wasn't digested with LSCM, we were able to measure the connective tissue area stained by Lucifer Yellow and evaluate the injury in the same exact location within the same tissue sample. Silica-induced granuloma formation, alveolar wall thickening, and infiltration of inflammatory cells in the air spaces of Lucifer Yellow-stained lung tissue were easily observed using LSCM. Lung tissue recovered from animals treated with saline and Fe_2O_3 appeared normal. Similar results were seen when the exposed tissue samples from the different treatment groups were stained with hematoxylin and eosin, a standard method of histological analysis. With LSCM, three-dimensional projection series of lung tissue 67.5–112.5 μm thick were easily generated that further confirmed the histological findings of the other procedures.

Using reflected light LSCM, we were also able to image deposited particles in the lungs. A significant amount of Fe_2O_3 was still present in the lungs 60 days post-instillation. Nearly all of these particles had aggregated together and accumulated in alveolar macrophages. This feature of LSCM may be extremely valuable in examining the toxicological response of the respiratory tract to inhaled fibrous and non-fibrous particles. Once a particle of fiber is deposited in the lungs, the residence time is an important determinant of toxicity (Davis *et al*., 1986). Since there is little physical disruption of the tissue with LSCM analysis, the distribution of inhaled particles can be assessed. With the three-dimensional capabilities of LSCM, fibers can be imaged in full profile, allowing for the length of the fibers, the estimated fiber burden in the entire lung as well as in the different pulmonary compartments, and the orientation of the fibers with different cell types to be determined *in situ*.

We have introduced the application of LSCM in the analysis of particle-induced pulmonary fibrosis. While quantitative LSCM can be labor intensive and requires expensive and specialized equipment that may not be available to some researchers, it does offer several advantages over traditional biochemical methods that have been used in the past. Since tissue specimens are optically sectioned with minimal physical disruption, we have found this method to be a quick and efficient way to process large areas of lung. The use of LSCM may also be helpful for evaluation of diseased tissue which has been banked away from previous studies or when large amounts of tissue cannot be allocated for biochemical analysis. Different areas of damage can be distinguished, and localized areas of injury can be assessed. LSCM analysis may allow for observation of connective tissue accumulation in different anatomic locations of the lungs, such as the alveolar region, airway walls, and pleura. LSCM may prove extremely useful in studying the toxicology of deposited fibrous and non-fibrous particles. Pulmonary deposition, translocation, persistence, and clearance of inhaled particles can be easily evaluated. The association then between the development of lung disease and the deposition of inhaled particles could also be assessed within the same tissue sample. Lastly, LSCM may prove to be an important tool in examining human lung-biopsy samples where biochemical hydroxyproline analysis is impossible.

REFERENCES

Antonini, J. M., Krishna Murthy, G. G., Rogers, R. A., Albert, R., Ulrich, G. D., and Brain, J. D. (1996). Pneumotoxicity and pulmonary clearance of different welding fumes after intratracheal instillation in the rat. *Toxicol. Appl. Pharmacol*. **140,** 188–199.

Beck, B. D., Brain, J. D., and Bohannon, D. E. (1982). An *in vivo* hamster bioassay to assess the toxicity of particulates for the lungs. *Toxicol. Appl. Pharmacol.* **66,** 9–29.

Blake, T. L., DiMatteo, M., Antonini, J. M., McCloud, C. M., and Reasor, M. J. (1996). Subchronic pulmonary inflammation and fibrosis induced by silica in rats are attenuated by amiodarone. *Exp. Lung Res*. **22,** 113–131.

Bowden, D. (1987). Macrophages, dust, and pulmonary diseases. *Exp. Lung Res*. **12,** 89–107.

Brain, J. D., Knudson, D. E., Sorokin, S. P., and Davis, M. A. (1976). Pulmonary distribution of particles given by intratracheal instillation or by aerosol inhalation. *Environ. Res*. **11,** 13–33.

Davis, J. M. G., Addison, J., Bolton, R. E., Donaldson, K., Jones, A. D., and Smith, T. (1986). The pathogenicity of long versus short fibre samples of amosite asbestos administered to rats by inhalation and intraperitoneal injection. *Br. J. Exp. Pathol*. **67,** 415–430.

Gil, J., Bachofen, H., Gehr, P., and Weibel, E. R. (1979). Alveolar volume-surface area relation in air- and saline-filled lungs fixed by vascular perfusion. *J. Appl. Physiol*. **47,** 990-1001.

Hakkinen, P. J., Morse, C. C., Martin, F. M., Dalbey, W. E., Haschek, W. M., and Witschi, H. P. (1983). Potentiating effects of oxygen in lungs damaged by methlcyclopentadienyl manganese tricarbonyl, cadmium chloride, oleic acid, and antitumor drugs. *Toxicol. Appl. Pharmacol.* **67,** 55–69.

Haschek, W. M., Klein-Szanto, A. J. P., Last, J. A., Reiser, K. M., and Witschi, H. P. (1982). Long-term morphologic and biochemical features of experimentally induced lung fibrosis in the mouse. *Lab. Invest*. **46,** 438–449.

Haschek, W. M., and Witschi, H. P. (1979). Pulmonary fibrosis: A possible mechanism. *Toxicol. Appl. Pharmacol*. **51,** 475–487.

Inoue, S. (1989). In *The Handbook of Biological Confocal Microscopy* (J. Pawley, Ed.). IMR Press, University of Wisconsin, Madison, WI.

Lapp, N. L., and Castranova, V. (1993). How silicosis and coal worker's pneumoconiosis develop- a cellular assessment. In *Occupational Medicine: State of Art Reviews- The Mining Industry* (D. E. Banks, Ed.), Vol. 8, No. 1. Hanley and Belfus, Philadelphia.

Malkusch, W., Rehn, B., and Bruch, J. (1995). Advantages of Sirius red staining for quantitative morphometric collagen measurements in lungs. *Exp. Lung Res*. **21,** 67–77.

Oldmixon, E. H., Brismar, H., Lai, J., Ekstein, B. A., and Rogers, R. A. (1994). Overcoming confocal scanning laser microscopy depth limitations. *FASEB J*. **8,** A691.

Oldmixon, E. H., and Carlsson, K. (1993). Methods for large data volumes from confocal scanning laser microscopy of lung. *J. Microsc*. **170,** 221–228.

Pawley, J. (1989). In *The Handbook of Biological Confocal Microscopy* (J. Pawley, Ed.). IMR Press, University of Wisconsin, Madison, WI.

Rogers, R. A., Oldmixon, E. H., and Brain, J. D. (1992). Enhanced contrast within embedded tissue by lucifer yellow CH: An ideal stain for laser scanning confocal microscopy. *Mol. Biol. Cell*. **3,** 185a.

Sferlazza, S. J., and Beckett, W. S. (1991). The respiratory health of welders. *Am. Rev. Respir. Dis*.**143,** 1134–1148.

Shotten, D. M. (1989). Confocal scanning optical microscopy and its applications for biological specimens. *J. Cell Sci*. **94,** 175–206.

Smith, G. J., Bagnell, C. R., Bakewell, W. E., Black, K. A., Bouldin, T. W., Earnhardt, T. S., Hook, G. E. R., and Pryzwansky, K. B. (1991). Application of confocal scanning laser microscopy in experimental pathology. *J. Electr. Microsc*. **18,** 38–49.

Valberg, P. A., and Brain, J. D. (1979). Generation and use of three types of iron-oxide aerosol. *Am. Rev. Respir. Dis*. **129,** 1013–1024.

Wilson, T. (1989). Trends in confocal microscopy. *Trends Neurosci*. **12,** 486–493.

Witschi, H. P., Tryka, A. F., and Lindenschmidt, R. C. (1985). The many faces of an increase in lung collagen. *Fundam. Appl. Toxicol*. **5,** 240–250.

Wright, S. J., Centonze, V. E., Stricker, S. A., DeVries, P. J., Paddock, S. W., and Schatten G. (1993). Introduction to confocal microscopy and three-dimensional reconstruction.In *Methods in Cell Biology* (B. Matsumoto, Ed.), Vol. 38, 1–45. Academic Press, New York.